AD-A286 383

AD

RESIDUAL STRESS ANALYSIS IN SWAGE AUTOFRETTAGED THICK-WALLED CYLINDERS BY POSITION-SENSITIVE X-RAY DIFFRACTION TECHNIQUES

S.L. LEE
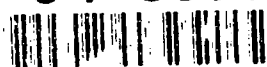
DTIC
ELECTE
NOV 21 1994
B

AUGUST 1994

US ARMY ARMAMENT RESEARCH, DEVELOPMENT AND ENGINEERING CENTER
CLOSE COMBAT ARMAMENTS CENTER
BENÉT LABORATORIES
WATERVLIET, N.Y. 12189-4050

94-35772

94 11 18 3

DISCLAIMER

The findings in this report are not to be construed as an official Department of the Army position unless so designated by other authorized documents.

The use of trade name(s) and/or manufacturer(s) does not constitute an official indorsement or approval.

DESTRUCTION NOTICE

For classified documents, follow the procedures in DoD 5200.22-M, Industrial Security Manual, Section II-19 or DoD 5200.1-R, Information Security Program Regulation, Chapter IX.

For unclassified, limited documents, destroy by any method that will prevent disclosure of contents or reconstruction of the document.

For unclassified, unlimited documents, destroy when the report is no longer needed. Do not return it to the originator.

REPORT DOCUMENTATION PAGE

Public reporting burden for this collection of information is estimated to average 1 hour per response, including the time for reviewing instructions, searching existing data sources, gathering and maintaining the data needed and completing and reviewing the collection of information. Send comments regarding this burden estimate or any other aspect of this collection of information, including suggestions for reducing this burden to Washington Headquarters Services, Directorate for Information Operations and Reports, 1215 Jefferson Davis Highway, Suite 1204, Arlington, VA 22202-4302 and to the Office of Management and Budget, Paperwork Reduction Project (0704-0188) Washington, DC 20503

1. AGENCY USE ONLY (Leave blank)	2. REPORT DATE	3. REPORT TYPE AND DATES COVERED
	August 1994	Final

4. TITLE AND SUBTITLE	5. FUNDING NUMBERS
RESIDUAL STRESS ANALYSIS IN SWAGE AUTOFRETTAGED THICK-WALLED CYLINDERS BY POSITION-SENSITIVE X-RAY DIFFRACTION TECHNIQUES	AMCMS: 6111.02.H611.1

6. AUTHOR(S)

S. L. Lee

7. PERFORMING ORGANIZATION NAME(S) AND ADDRESS(ES)	8. PERFORMING ORGANIZATION REPORT NUMBER
U.S. Army ARDEC Benet Laboratories, SMCAR-CCB-TL Watervliet, NY 12189-4050	ARCCB-TR-94031

9. SPONSORING/MONITORING AGENCY NAME(S) AND ADDRESS(ES)	10. SPONSORING/MONITORING AGENCY REPORT NUMBER
U.S. Army ARDEC Close Combat Armaments Center Picatinny Arsenal, NJ 07806-5000	

11. SUPPLEMENTARY NOTES

12a. DISTRIBUTION/AVAILABILITY STATEMENT	12b. DISTRIBUTION CODE
Approved for public release; distribution unlimited.	

13. ABSTRACT (Maximum 200 words)

Experimental and theoretical investigations were made for swage autofrettaged partially plastic ASTM A723 steel cylinders with an outside diameter (OD) to inside diameter (ID) ratio of 2.75 and 74 percent overstrain. Residual stress radial distribution and angular stress distribution around the bore were analyzed using two position-sensitive x-ray diffraction stress analyzers. Theoretical calculation was made by implementing an interactive, iterative Lotus Works spreadsheet residual stress model on an IBM PC. The model was based on the classical solution to the elastic-plastic deformation problem of a symmetric thick-walled cylinder under internal pressure, including reverse yielding effect. Angular stress distribution data at the ID and OD indicated that non-axisymmetric deformation had occurred during yielding of the cylinders. Excellent agreement was obtained between experimental results and theoretical predictions, including the Bauschinger effect near the bore. By comparing experimental data with theoretical calculations for the 74 percent overstrained cylinders, the Bauschinger factor for the A723 steel was determined to be close to 0.5. Residual stress analysis for the entire cylinder is suggested in the future.

14. SUBJECT TERMS Residual Stress, Swage Autofrettage, Bauschinger's Effect, Position-Sensitive Stress Analyzer, X-Ray Diffraction, Pressure Vessel, Reverse Yielding, Plastic Deformation			15. NUMBER OF PAGES 15
			16. PRICE CODE

17. SECURITY CLASSIFICATION OF REPORT	18. SECURITY CLASSIFICATION OF THIS PAGE	19. SECURITY CLASSIFICATION OF ABSTRACT	20. LIMITATION OF ABSTRACT
UNCLASSIFIED	UNCLASSIFIED	UNCLASSIFIED	UL

NSN 7540-01-280-5500

TABLE OF CONTENTS

Tables

List of Illustrations

Distribution

Availability Codes

Dist | Avail and/or
     | Special

A-1

i

INTRODUCTION

It is a well-known fact that nearly all fatigue and stress corrosion failures originate at the surface of a part, and that cracks do not propagate into a compressed layer of a component. Autofrettage, shot peen, and shrink fit are common processes to induce compressive stresses near the bore surface of a cylinder. In the manufacturing of high pressure vessel systems, steel cylinders made from ASTM A723 alloys are rotary forged, heat hardened through austenizing and quenching processes, tempered to improve toughness, rough and fine machined, swage autofrettaged, beam straightened, and thermally soaked to obtain desirable residual stress distributions.

Excellent earlier developmental work for hydraulic and mechanical swage autofrettage manufacturing processes were reported (refs 1,2). The hydraulic autofrettage process was slow, expensive, and dangerous. High pressures close to failure in the range of 1000 to 2000 mpa were necessary. By driving a mandrel through the cylinder, the swage process eliminated the necessity of ultrahigh pressures required in the conventional hydraulic method to produce the same radial forces and plastic deformation. Davidson and Kendall further reported results of residual stress investigation in swaged cylinders by Sack's boring out method (ref 3). Clark observed variations in hoop residual stresses for a large caliber gun barrel forging (ref 4). Parker et al. studied the fatigue crack growth and safe design of gun tubes (ref 5). Results from our x-ray diffraction and finite element modeling investigation of an eccentric cylinder were reported (refs 6,7). Interest in the Bauschinger effect in thick-walled cylinders is obvious (8-11), since there is little experimental data available.

With the recent development of position-sensitive x-ray diffraction instrumentation, fast and reliable stress measurements are possible. The present work characterized residual stress distribution in a symmetric pre-pressurized partially plastic thick-walled cylinder by swage autofrettage. Comparison of the present theoretical calculation with our previous data for an eccentric cylinder of the same dimension was made. Measurements were made using both a position-sensitive single-exposure scintillation detection (PSSD) system and a position-sensitive multiple-exposure proportional counter stress analyzer. Angular stress distribution measurements around the bore indicated that non-axisymmetric deformation had occurred during yielding of a symmetric cylinder.

Theoretical residual stress predictions were made assuming a classical model of a symmetric cylinder under internal pressure. An iterative Lotus Works spreadsheet residual stress program based on Parker's model (ref 5) was designed and implemented on an IBM PC. Excellent agreement was found between experimental and theoretical results, including the Bauschinger effect near the bore. The Bauschinger factor is defined as the ratio of yield strength in compression to yield strength in tension. It can be described as a lowering of the elastic limit in compression subsequent to a previous stressing in tension beyond the elastic limit. Conversely, the elastic limit in tension would be reduced for a material strained beyond the elastic limit in compression (ref 11). A qualitative comparison of our experimental data for the 74 percent overstrained tube with model calculations indicated that the Bauschinger factor for the A723 steel was close to 0.5.

1

SPECIMEN PREPARATION

In the swage process, the cylinder was subjected to plastic deformation by pushing an oversized mandrel through the bore under high pressure grease. Material constant, geometry of the ram, mandrel, and cylinder, and the shape and interference of the carbide tool determine the amount of plastic deformation under load. The thick-walled cylinder investigated was 74 percent overstrained with an OD to ID ratio of 2.75. Slices of the tube 3.79 cm (1.5 in.) thick were cut from the cylinder, machine polished, and then electropolished. Electropolishing of the entire cross section of the ring was done by using a heated polishing solution of 50 percent sulfuric and 50 percent phosphoric acid mixture with no external agitation device. It took approximately one hour to remove 0.13 mm (5 mils) from the surface of the ring. Surface material removal was made so that the effects due to sanding, machining, and oxidation would not influence the residual stress measurements.

EXPERIMENTAL METHOD

Experimental analyses were made using both a prototype PSSD system from Denver X-Ray Instruments, and a position-sensitive multiple-exposure proportional counter stress analyzer from Technology for Energy Corp (TEC). Experimental methods and calibration of the Denver stress analyzer have been described in another report (ref 12). The K-α from a chromium x-ray tube reflects from the 211 plane of the body-centered-cubic (BCC) steel at 2θ equal to 156.41 degrees. The fast single-exposure method was used in the radial stress distribution analysis; the accurate multiple-exposure method was used to analyze hoop and radial angular stress distribution around the bore.

The choice of zero degree for a normal cylinder was arbitrary. The surface was marked into 32 equal area pie slices at an 11.25-degree span each. For stress distribution determination analysis, a specimen stage with an x- and y-micrometer slide was used. Angular stress variation measurements were made by manually rotating and positioning the specimen. Symphony, Lotus Works, and Freelance software were used for data analysis and graphics.

X-RAY DIFFRACTION HOOP STRESS RADIAL DISTRIBUTION ANALYSIS

In Figure 1, the x-ray diffraction experimental hoop residual stress radial distributions along radii at 0, 90, 180, and 270 degrees for a symmetric swaged cylinder are displayed. Experimental x-ray diffraction results for the swaged cylinders exhibited compressive residual stresses near the bore; the stresses gradually changed to tensile stresses near the outside surface of the cylinder. Closest to the bore, reduced compressive stresses were observed in all measurements. The solid curve in the figure represents the average stress from 0, 90, 180, and 270 degree stress measurements in the symmetric cylinder.

2

X-RAY DIFFRACTION ANGULAR STRESS DISTRIBUTION

In Figure 2, hoop and radial stresses at the ID and OD of a symmetric swaged cylinder at various angular positions are plotted. Angular stress data showed a peak of reduced compressive stress around a random 290 degree plot. The data are in good agreement with Figure 1, where the 270 degree plot has less compressive stress near the bore. Hoop and radial stresses at the ID and OD of an eccentric cylinder with an 0.1-inch wall thickness variation measured on a TEC position-sensitive multiple-exposure stress analyzer have been reported (refs 6,7). A peak of reduced compressive stress was observed around 180 degrees, which was the thinnest part of the eccentric cylinder. It is surprising to find non-uniform stress distribution in both a symmetric and an eccentric cylinder. Possible causes for this non-axisymmetric yielding are variations in material properties, non-uniform heat treatment procedure, eccentricity, tribological problems, non-axisymmetric processing, unknown effects during manufacturing, or a combination of these factors. Another observation is that the radial stresses at the ID and OD are near zero for the symmetric cylinder, as expected from Tresca's theoretical predictions shown in the next section. OD radial stresses for the eccentric cylinder peaked around 0 degree, which is the thickest part of the cylinder.

CLASSICAL ELASTIC-PLASTIC DEFORMATION MODEL CALCULATIONS

In the autofrettage process due to internal loading, the bore is plastically enlarged, and the outer portion of the steel cylinder is elastically enlarged. As the internal pressure p is released, the outer portion contracts elastically to its original dimension; steel nearer the bore resists this action. This results in compressive hoop residual stresses near the bore that changes to tensile stress near the outer surface. However, closest to the bore, the Bauschinger effect causes reversed plasticity and reduces the compressive stresses.

To obtain theoretical stress predictions, a fast and versatile iterative Lotus Works spreadsheet program was designed and implemented on an IBM PC. Assuming a thick-walled cylinder overstrained by direct internal pressure, our analysis was based on Parker's solution to the classical elastic-plastic deformation problem using Lamé's equations, Tresca's yield criteria, and reverse yielding (ref 5). Figure 3 is a stress-strain curve used in the analysis that assumed an elastic-perfectly plastic behavior during loading, and reduced yield stress during unloading. The Bauschinger factor is given by α. Figure 4 is a cross-sectional display of a pre-pressurized autofrettaged cylinder after internal pressure has been removed, showing regions of elasticity, elastic-plastic interface, and reversed plasticity. The inside radius is a, the outside radius is b, the elastic-plastic interface radius is c, and the reversed plasticity radius is d. Table 1 gives the equations used in the model. In Figure 5, predicted residual stress distributions are given for Bauschinger factor α equal to 0.25, 0.5, and 0.75. The calculation assumed a yield stress of 162 Ksi.

3

Variable radius- r   Elastic-plastic interfaces- c,d
Inside radius- a   Interface pressure at c- p^*
Outside radius- b   Interface pressure at d- p
Yield strength- Y
Bauschinger factor- α
Hoop stress- σ_θ
Radial stress- σ_r

Region of reverse plasticity, a < r < d

$$\sigma_\theta = -\alpha Y (1 + \ln (r/a))$$

$$\sigma_r = -\alpha Y \ln (r/a)$$

Region of plasticity, d < r < c

$$\sigma_\theta^T = - \left\{ p^* - (1 + \alpha) Y \ln (d/a) \right\} \frac{d^2}{b^2-d^2} \left[1 + \frac{b^2}{r^2} \right] - p^* + Y (1 + \ln (r/a))$$

$$\sigma_r^T = - \left\{ p^* - (1 + \alpha) Y \ln (d/a) \right\} \frac{d^2}{b^2-d^2} \left[1 - \frac{b^2}{r^2} \right] - p^* + Y \ln (r/a)$$

Region of elasticity, c < r < b

$$\sigma_\theta^T = \left[1 + \frac{b^2}{r^2} \right] \left[\frac{Yc^2}{2b^2} - \left\{ p^* - (1 + \alpha) Y \ln (d/a) \right\} \frac{d^2}{b^2-d^2} \right]$$

$$\sigma_r^T = \left[1 - \frac{b^2}{r^2} \right] \left[\frac{Yc^2}{2b^2} - \left\{ p^* - (1 + \alpha) Y \ln (d/a) \right\} \frac{d^2}{b^2-d^2} \right]$$

$$p^* = Y \ln (c/a) + \frac{Y}{2b^2} (b^2 - c^2)$$

$$-p = \sigma_r \big|_{r=d} = p^* - (1 + \alpha) Y \ln (d/a)$$

COMPARISON OF EXPERIMENTAL STRESSES WITH CALCULATIONS

In Figure 6, experimental residual stress distributions for a symmetric cylinder displayed as data points are compared with theoretical stresses for α equal to 0.5 displayed as solid curves. Excellent agreement was observed, indicating that the Bauschinger factor for A723 steel was close to 0.5. The deviations between experimental and calculated results were the largest at 270 degrees because of the non-uniform stress distribution in this region. A qualitative comparison of the present experimental results with Chen's numerical residual stresses including Bauschinger and strain-hardening effects upon unloading (ref 10) indicated that the strain-hardening factor m' was near 0, and the Bauschinger factor α was between 0.4 and 1.0. As shown in Figure 7, Milligan determined that for martensite structure, the Bauschinger factor for permanent tensile overstrain over 2 percent is approximately 0.35. This is in fair agreement with our determination of $\alpha = 0.5$.

In Figure 8, theoretical stresses for α equal to 0.5 represented in solid lines are compared with our previous residual stress measurements of an eccentric cylinder plotted as data points. Again, excellent agreement was observed between experimental and theoretical hoop and radial stresses. The large deviations at 180 degrees, where the cylinder was the thinnest, may be due to material property variations, eccentricity, or other factors.

Since residual stresses must form a balanced force system within the object, a slight shift of the experimental stress distribution curves would render better agreement with calculations. This could be experimentally accounted for by zero powder stress corrections to the experimental results. Moreover, the difference in the nature of the induced stress conditions by the swage process as compared to the internal pressurization method should result in some differences in the stress distributions.

CONCLUSIONS

Stress analysis of swaged components provides guidance to the pressure vessel system's design. This is because controlled stress distribution improves the system's performance and fatigue life of the component. In this work, position-sensitive x-ray diffraction techniques were applied to characterize residual stresses in pre-pressurized thick-walled swaged autofrettaged cylinders. Excellent agreement was obtained with theoretical predictions obtained by assuming a classical elastic-plastic deformation model including reverse yielding effect. For the 74 percent overstrained cylinder, qualitative comparison of our experimental results with theoretical calculations determined that the Bauschinger factor for the A723 steel was 0.5. The non-uniform bore stress distribution around the random 290 degrees should be further investigated for manufacturing quality control purposes. Suggested future investigations include an improved finite element swage model, an analytical elastic-plastic deformation swage model, and experimental investigations in residual stress, strain attenuation, hardness, and phase transformation in the entire cylinder.

REFERENCES

1. T.E. Davidson, C.S. Barton, A.N. Reiner, and D.P. Kendall, "Overstrain of High Strength, Open End Cylinders of Intermediate Diameter Ratio," *First International Congress on Experimental Mechanics*, Pergamon Press, Oxford, 1963, pp. 335-352.

2. T.E. Davidson, C.S. Barton, A.N. Reiner, and D.P. Kendall, "New Approach to the Autofrettage of High-Strength Cylinders," *Experimental Mechanics*, 1962, pp. 33-40.

3. T.E. Davidson, and D.P. Kendall, "Residual Stresses in Thick-Walled Cylinders Resulting From Mechanically-Induced O erstrain," *Experimental Mechanics*, November, 1963, pp. 253-262.

4. G. Clark, "Residual Stresses in Swage-Autofrettaged Thick-Walled Cylinders," Materials Research Laboratories Report MRL-R-847, 1982.

5. A.P. Parker, K.A. Sleeper, and C.P. Andrasic, "Safe Life Design of Gun Tubes--Some Numerical Methods and Results," *Proceedings of the Army Numerical Analysis and Computer Conference*, 1981, pp. 311-333.

6. S.L. Lee, G.P. O'Hara, V. Olmstead, and G. Capsimalis, "Characterization of Residual Stresses in an Eccentric Swage Autofrettaged Thick-Walled Cylinder," *Proceedings of the ASM International Conference on the Practical Applications of Residual Stress Technology*, 1991, pp. 123-129.

7. S.L. Lee, L. Britt, and G. Capsimalis, "Comparison of Residual Stress and Hardness in a Symmetric and an Eccentric Swage Autofrettaged Cylinder," *Nondestructive Characterization of Materials VI*, to be published.

8. D.P. Kendall, "The Influence of the Bauschinger Effect on Re-Yielding of Autofrettaged Thick-Walled Cylinders," ASME Special Publication PVP Vol. 125, 1987, pp. 17-21.

9. J. He, G. Chen, H. Zhong, "The Influence of Strain Hardening and Bauschinger Effect Behavior of the Material on the Autofrettage Residual Stresses of a Thick-Walled Cylinder," ASME Special Publication PVP-Vol. 110, 1986, pp 49-54.

10. P.C.T. Chen, "Stress and Deformation Analysis of Autofrettaged High Pressure Vessels," ASME Special Pub. PVP-Vol. 110, 1986, pp. 61-67.

11. R.V. Milligan, W.H. Koo, and T.E. Davidson, "The Bauschinger Effect in a High Strength Steel," Trans. ASME, Series D, June 1966, pp. 480-488.

12. S.L. Lee, M. Doxbeck, and G. Capsimalis, "X-Ray Diffraction Study of Residual Stresses in Metal Matrix Composite-Jacketed Steel Cylinder Subjected to Internal Pressure," *Nondestructive Characterization of Materials IV*, 1992, pp. 419-427.
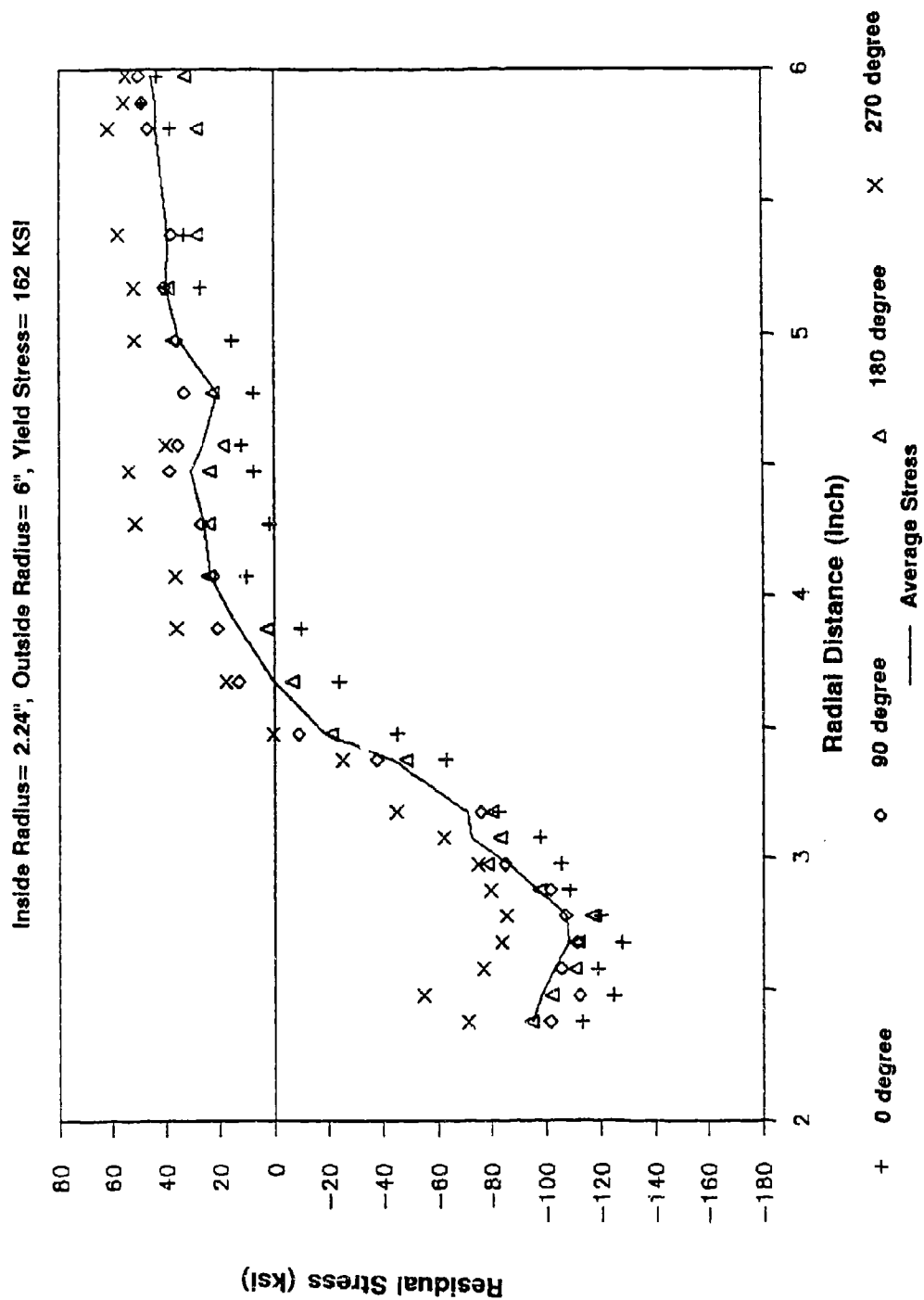
Figure 1. Hoop residual stress distribution in a symmetric cylinder.
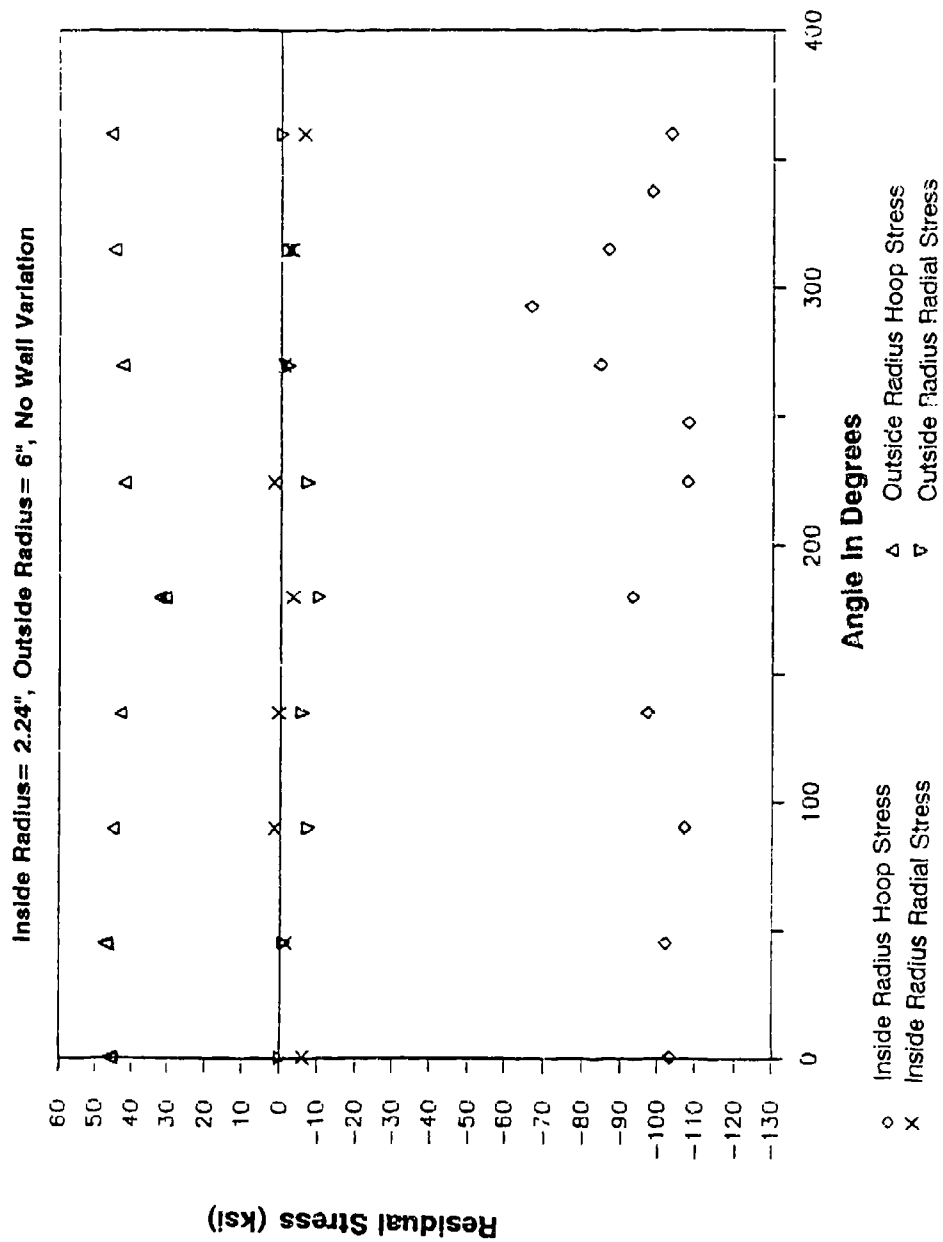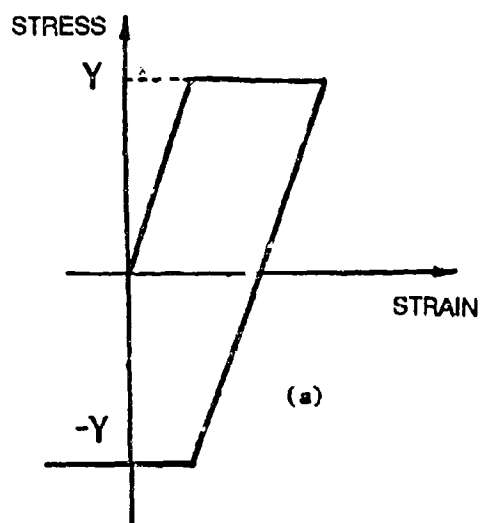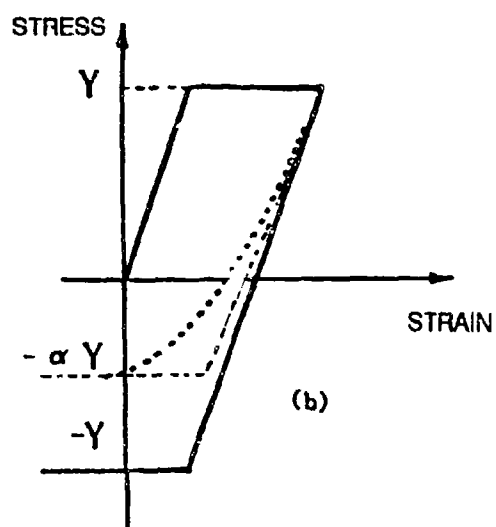
Figure 2. Residual stress angular variation in a symmetric cylinder.

STRESS

Y

STRAIN

(a)

-Y

STRESS

Y

STRAIN

- α Y

(b)

-Y

ELASTIC-PERFECTLY PLASTIC:

YIELD STRESS IN TENSION EQUALS
YIELD STRESS IN COMPRESSION.

BAUSCHINGER EFFECT:

REDUCED YIELD STRESS IN COMPRESSION,
BAUSCHINGER FACTOR DEFINED AS ALPHA.

Figure 3. Theoretical stress-strain curve for A723 steel.

9

a= Inside Radius, b= Outside Radius,
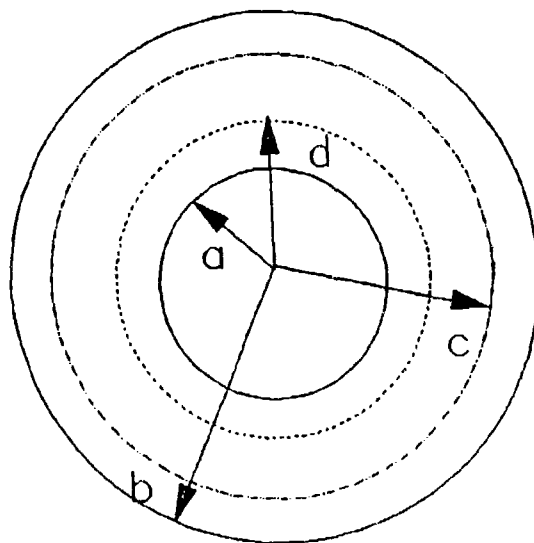c= Elastic-Plastic Interface Radius, d= Reversed Plasticity Radius

Figure 4. Pressurized cylinder after removal of internal pressure.
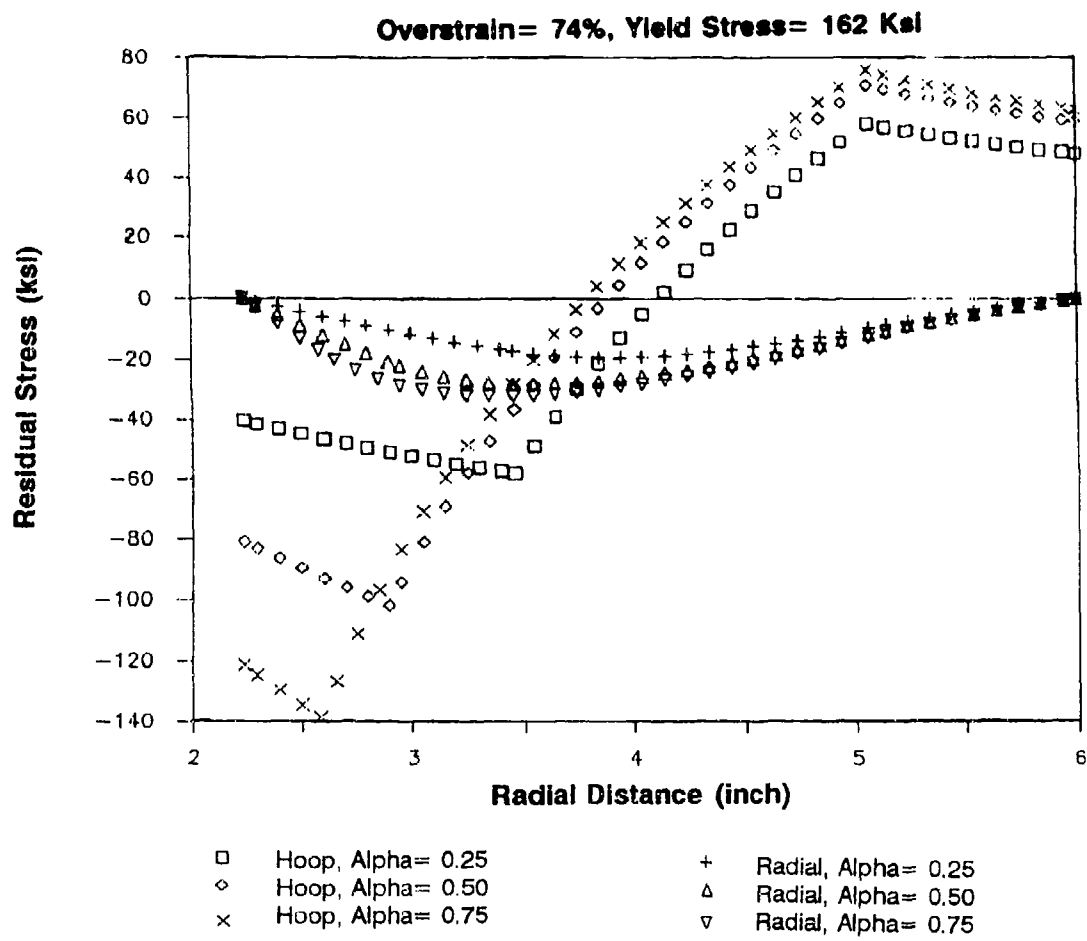
Overstrain= 74%, Yield Stress= 162 Ksi

Figure 5. Classical theoretical hoop and radial stress distribution.

11

Figure 6. Experimental and classical deformation model stresses
including reverse yielding in a symmetric cylinder.

12

BEF VS PERCENT TENSILE OVERSTRAIN
VARIOUS STRUCTURES

A- MARTENSITIC STRUCTURE (YIELD STRESS=160 KSI)
B- BAINITIC STRUCTURE
C- PEARLITIC STRUCTURE

BEF

1.0
0.9
0.8
0.7
0.6
0.5
0.4
0.3
0.0

0   1   2   3   4   5

PERCENT TENSILE OVERSTRAIN

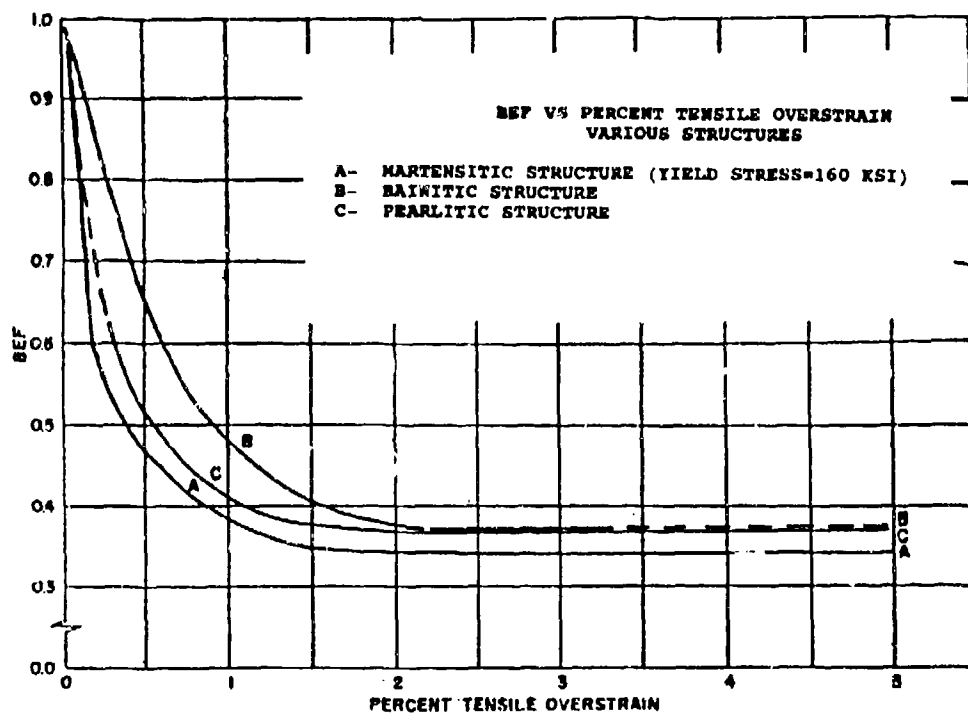Figure 7. Bauschinger effect factor (BEF) versus percent tensile overstrain (ref 11).
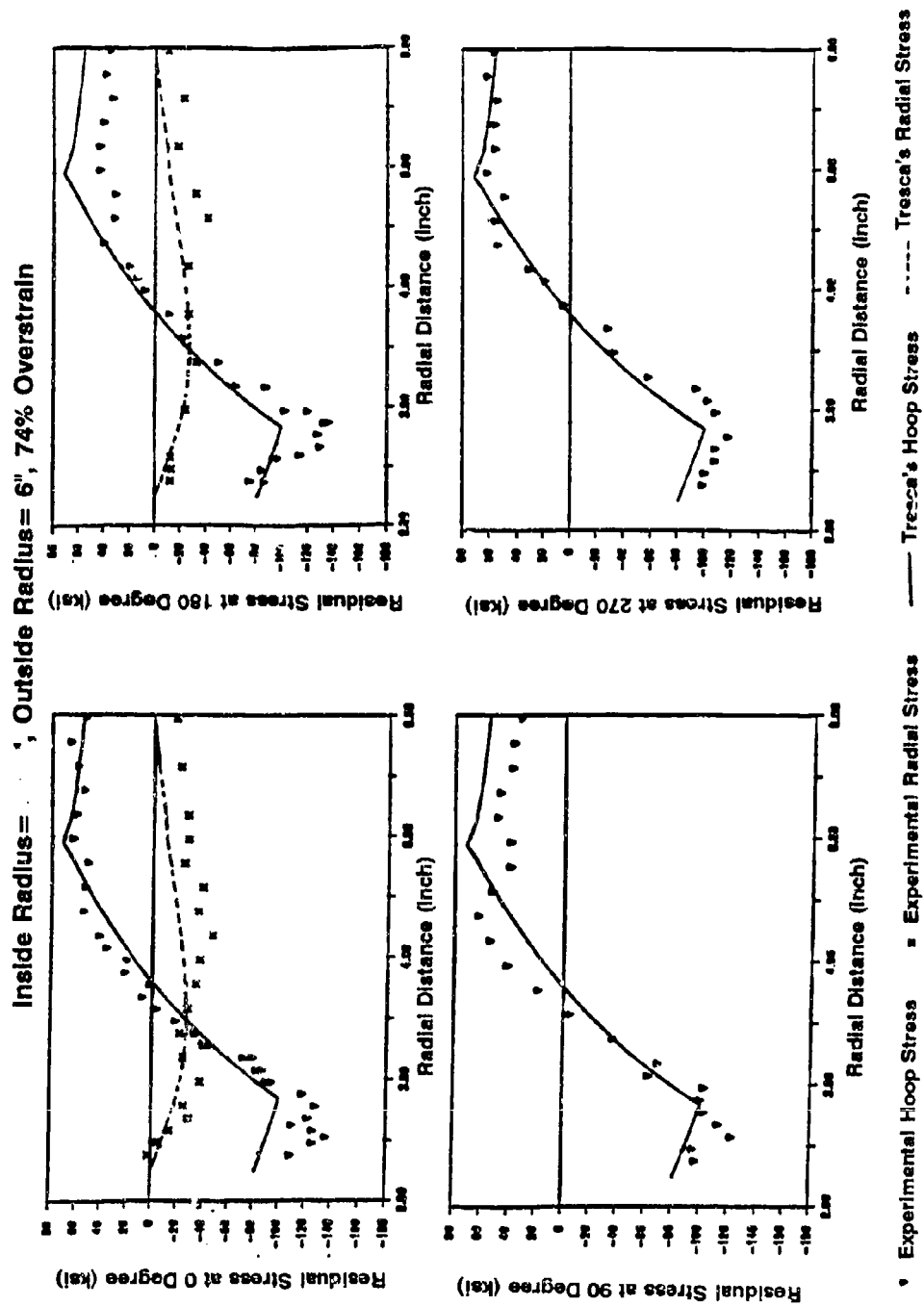
13

Figure 8. Experimental and classical deformation model stresses including reverse yielding in an eccentric cylinder.

14

TECHNICAL REPORT INTERNAL DISTRIBUTION LIST

	NO. OF COPIES
CHIEF, DEVELOPMENT ENGINEERING DIVISION	
ATTN: SMCAR-CCB-DA	1
-DC	1
-DI	1
-DR	1
-DS (SYSTEMS)	1
CHIEF, ENGINEERING DIVISION	
ATTN: SMCAR-CCB-S	1
-SD	1
-SE	1
CHIEF, RESEARCH DIVISION	
ATTN: SMCAR-CCB-R	2
-RA	1
-RE	1
-RM	1
-RP	1
-RT	1
TECHNICAL LIBRARY	
ATTN: SMCAR-CCB-TL	5
TECHNICAL PUBLICATIONS & EDITING SECTION	
ATTN: SMCAR-CCB-TL	3
OPERATIONS DIRECTORATE	
ATTN: SMCWV-ODP-P	1
DIRECTOR, PROCUREMENT & CONTRACTING DIRECTORATE	
ATTN: SMCWV-PP	1
DIRECTOR, PRODUCT ASSURANCE & TEST DIRECTORATE	
ATTN: SMCWV-QA	1

NOTE: PLEASE NOTIFY DIRECTOR, BENÉT LABORATORIES, ATTN: SMCAR-CCB-TL OF ADDRESS CHANGES.

TECHNICAL REPORT EXTERNAL DISTRIBUTION LIST

	NO. OF COPIES		NO. OF COPIES

ASST SEC OF THE ARMY
RESEARCH AND DEVELOPMENT
ATTN: DEPT FOR SCI AND TECH   1
THE PENTAGON
WASHINGTON, D.C. 20310-0103

ADMINISTRATOR
DEFENSE TECHNICAL INFO CENTER   12
ATTN: DTIC-FDAC
CAMERON STATION
ALEXANDRIA, VA 22304-6145

COMMANDER
U.S. ARMY ARDEC
ATTN: SMCAR-AEE   1
    SMCAR-AES, BLDG. 321   1
    SMCAR-AET-O, BLDG. 351N   1
    SMCAR-FSA   1
    SMCAR-FSM-E   1
    SMCAR-FSS-D, BLDG. 94   1
    SMCAR-IMI-I, (STINFO) BLDG. 59   2
PICATINNY ARSENAL, NJ 07806-5000

DIRECTOR
U.S. ARMY RESEARCH LABORATORY
ATTN: AMSRL-DD-T, BLDG. 305   1
ABERDEEN PROVING GROUND, MD
  21005-5066

DIRECTOR
U.S. ARMY RESEARCH LABORATORY
ATTN: AMSRL-WT-PD (DR. B. BURNS)   1
ABERDEEN PROVING GROUND, MD
  21005-5066

DIRECTOR
U.S. MATERIEL SYSTEMS ANALYSIS ACTV
ATTN: AMXSY-MP   1
ABERDEEN PROVING GROUND, MD
  21005-5071

COMMANDER
ROCK ISLAND ARSENAL
ATTN: SMCRI-ENM   1
ROCK ISLAND, IL 61299-5000

MIAC/CINDAS
PURDUE UNIVERSITY
P.O. BOX 2634   1
WEST LAFAYETTE, IN 47906

COMMANDER
U.S. ARMY TANK-AUTMV R&D COMMAND
ATTN: AMSTA-DDL (TECH LIBRARY)   1
WARREN, MI 48397-5000

COMMANDER
U.S. MILITARY ACADEMY
ATTN: DEPARTMENT OF MECHANICS   1
WEST POINT, NY 10966-1792

U.S. ARMY MISSILE COMMAND
REDSTONE SCIENTIFIC INFO CENTER   2
ATTN: DOCUMENTS SECTION, BLDG. 4484
REDSTONE ARSENAL, AL 35898-5241

COMMANDER
U.S. ARMY FOREIGN SCI & TECH CENTER
ATTN: DRXST-SD   1
220 7TH STREET, N.E.
CHARLOTTESVILLE, VA 22901

COMMANDER
U.S. ARMY LABCOM
MATERIALS TECHNOLOGY LABORATORY
ATTN: SLCMT-IML (TECH LIBRARY)   2
WATERTOWN, MA 02172-0001

COMMANDER
U.S. ARMY LABCOM, ISA
ATTN: SLCIS-IM-TL   1
2800 POWER MILL ROAD
ADELPHI, MD 20783-1145

NOTE: PLEASE NOTIFY COMMANDER, ARMAMENT RESEARCH, DEVELOPMENT, AND ENGINEERING CENTER, U.S. ARMY AMCCOM, ATTN: BENÉT LABORATORIES, SMCAR-CCB-TL, WATERVLIET, NY 12189-4050 OF ADDRESS CHANGES.

	NO. OF COPIES		NO. OF COPIES

COMMANDER
U.S. ARMY RESEARCH OFFICE
ATTN: CHIEF, IPO 1
P.O. BOX 12211
RESEARCH TRIANGLE PARK, NC 27709-2211

DIRECTOR
U.S. NAVAL RESEARCH LABORATORY
ATTN: MATERIALS SCI & TECH DIV 1
  CODE 26-27 (DOC LIBRARY) 1
WASHINGTON, D.C. 20375

COMMANDER
AIR FORCE ARMAMENT LABORATORY
ATTN: AFATL/MN 1
EGLIN AFB, FL 32542-5434

COMMANDER
AIR FORCE ARMAMENT LABORATORY
ATTN: AFATL/MNF 1
EGLIN AFB, FL 32542-5434

NOTE: PLEASE NOTIFY COMMANDER, ARMAMENT RESEARCH, DEVELOPMENT, AND ENGINEERING CENTER, U.S. ARMY AMCCOM, ATTN: BENÉT LABORATORIES, SMCAR-CCB-TL, WATERVLIET, NY 12189-4050 OF ADDRESS CHANGES.